

DYNAMIC ANALYSIS OF THICK PLATES SUBJECTED TO EARTQUAKE

ÖZDEMİR Y. I, AYVAZ Y.

Posta Adresi: Department of Civil Engineering, Karadeniz Technical University, 61080 Trabzon, TURKEY

E-posta: yaprakozdemir@hotmail.com

Keywords: Earthquake, thick plate, Mindlin's theory, finite element method, thickness/span ratio, aspect ratio, boundary conditions.

ABSTRACT *The purpose of this paper is to study shear locking-free analysis of thick plates using Mindlin's theory and to determine the effects of the thickness/span ratio, the aspect ratio and the boundary conditions on the linear responses of thick plates subjected to earthquake excitations. Finite element formulation of the equations of the thick plate theory is derived by using second order displacement shape functions. A computer program using finite element method is coded in C++ to analyze the plates clamped or simply supported along all four edges. Graphs are presented that should help engineers in the design of thick plates subjected to earthquake excitations. It is concluded that, in general, the thickness/span ratio is more effective on the maximum responses than the aspect ratio.*

INTRODUCTION

The plate theories differ from each other according to the assumptions concerning the rotation of normal direction on the middle surface. In the classical plate theory which is known as Kirchhoff Theory, normal direction of the thin plates remain straight and orthogonal when the plate is bent. However, the Reissner-Mindlin plate theories conserve the straight strain state of the normal direction, but do not demand it to be orthogonal with the strain of the middle surface.

Reissner (1947) derived expressions for moments and shear forces for isotropic elastic plates including the effects of shear deformation, rotatory inertia, and vertical stress σ_z by using a variational principle. Later Mindlin (1951) derived equations of motion for isotropic elastic plates including the effects of shear deformation and rotatory inertia and obtained the equations to calculate stresses of a plate. Ayvaz (1992) derived the equations of motions for orthotropic elastic plates using Hamilton's principle, but did not present any results. Özdemir and Ayvaz (2004) analyzed thick slabs with 4-noded finite element by using Mindlin's theory.

The purpose of this paper is to study shear locking-free analysis of thick plates using Mindlin's theory and to determine the effects of the thickness/span ratio, the aspect ratio and the boundary conditions on the linear responses of thick plates subjected to earthquake excitations. A computer program using finite element method is coded in C++ to analyze the plates clamped or simply supported along all four edges. In the program, the finite element method is used for spatial integration and the Newmark- β method is used for time integration. In the analysis, 8-noded finite elements are used to construct the stiffness and mass matrices since this element is free of the shear-locking problem (Özdemir et al., 2007).

Mathematical Model

The governing equation for a plate subjected to an earthquake excitation with no damping can be given as

$$[M]\{\ddot{w}\} + [K]\{w\} = -[M]\{\ddot{u}_g\} \quad (1)$$

where $[K]$ and $[M]$ are the stiffness matrix and the mass matrix of the plate, respectively, w and \ddot{w} are the lateral displacement and the second derivative of the lateral displacement of the plate with respect to time, respectively, and \ddot{u}_g is the earthquake acceleration.

Total Strain Energy of Plate

Total strain energy for a structural system can be written as

$$\Pi = \Pi_p + V, \quad (2)$$

where Π_p , the strain energy in the plate, is given as

$$\Pi_p = \frac{1}{2} \iiint_V \varepsilon^T \sigma dV \quad (3)$$

$$\Pi_p = \frac{1}{2} \int_{\Omega} \left(-\frac{\partial \varphi_x}{\partial x} \quad \frac{\partial \varphi_y}{\partial y} \quad -\frac{\partial \varphi_x}{\partial y} + \frac{\partial \varphi_y}{\partial x} \quad -\varphi_x + \frac{\partial w}{\partial x} \quad \varphi_y + \frac{\partial w}{\partial y} \right) [D] \begin{pmatrix} -\frac{\partial \varphi_x}{\partial x} \\ \frac{\partial \varphi_y}{\partial y} \\ -\frac{\partial \varphi_x}{\partial y} + \frac{\partial \varphi_y}{\partial x} \\ -\varphi_x + \frac{\partial w}{\partial x} \\ \varphi_y + \frac{\partial w}{\partial y} \end{pmatrix} dx dy \quad (4)$$

and V , the potential energy of the earthquake loading, is written as follows:

$$V = - \int_{\Omega} \bar{q} w dx dy. \quad (5)$$

In these equations, D is the flexural rigidity of the plate, x , y , and z are the coordinate axes as shown in Figure 1, Ω is the domain of the plate, and \bar{q} denotes

$$-[M]\{\ddot{u}_g\} \quad (6)$$

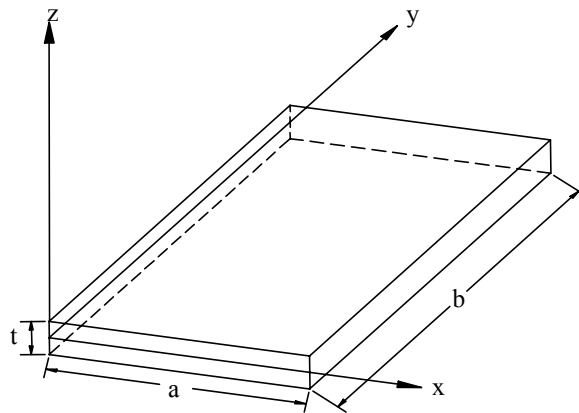


Figure 1. The plate used in this study

Matrix [D] may be partitioned into;

$$D = \begin{bmatrix} E_k & 0 \\ 0 & E_\gamma \end{bmatrix} \quad (7)$$

in which $[E_k]$ is of size 3x3 and $[E_\gamma]$ is of size 2x2. $[E_k]$, and $[E_\gamma]$ can be written as follows [10]:

$$[E_k] = \frac{t^3}{12} \begin{bmatrix} \frac{E}{(1-\nu^2)} & \frac{\nu E}{(1-\nu^2)} & 0 \\ \frac{\nu E}{(1-\nu^2)} & \frac{E}{(1-\nu^2)} & 0 \\ 0 & 0 & \frac{E}{2(1-\nu)} \end{bmatrix}; \quad [E_\gamma] = k t \begin{bmatrix} \frac{E}{2.4(1+\nu)} & 0 \\ 0 & \frac{E}{2.4(1+\nu)} \end{bmatrix}. \quad (8)$$

In this equation, t is the thickness of the plate, k is a constant to account for the actual nonuniformity of the shearing stresses.

Stiffness Matrix

The simplest type of plate-bending element has rectangular geometry which is a special case of quadrilateral geometry. In this study, one kind of serendipity elements, 8-noded quadrilateral element (QPBE8) is used (Figure 2).

The nodal displacements for this element can be written as follows;

$$u = \{u, v, w\} = \{-z\phi_x, z\phi_y, w\} = \left\{ -z \frac{\partial \phi_i}{\partial x}, z \frac{\partial \phi_i}{\partial y}, w \right\} \quad (9)$$

$$u = -z\phi_x = -z \sum_{i=1}^8 h_i \phi_{xi}, \quad v = z\phi_y = z \sum_{i=1}^8 h_i \phi_{yi}, \quad w = \sum_{i=1}^8 h_i w_i \quad (10)$$

The displacement function chosen for this element is ;

$$w = c_1 + c_2r + c_3s + c_4r^2 + c_5rs + c_6s^2 + c_7r^2s + c_8rs^2 \quad (11)$$

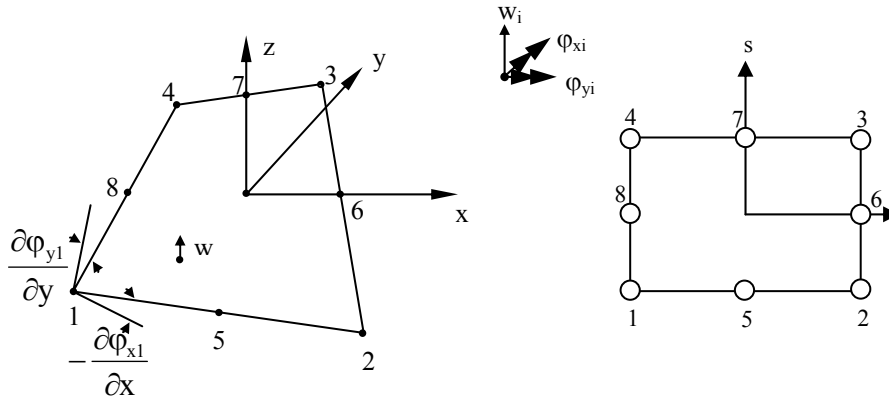


Figure 2. 8-noded quadrilateral element used in this study

From this assumption, it is possible to derive the displacement shape function to be;

$$h = [h_1, h_2, h_3, h_4, h_5, h_6, h_7, h_8]. \quad (12)$$

For more information about these matrices, see reference (Weaver and Jahston, 1984).

Before formulating element stiffness matrix, strain-displacement matrix B is partitioned as follows:

$$[B] = \begin{bmatrix} B_k \\ B_\gamma \end{bmatrix} = \begin{bmatrix} z\bar{B}_k \\ B_\gamma \end{bmatrix}. \quad (13)$$

Where B_k has the size of 3×24 and B_γ has the size of 2×24 , respectively. Then the stiffness matrices for this element is written as (Cook, 1989),

$$K = \int_A \bar{B}^T \bar{E} \bar{B} dA = \int_{-1}^1 \int_{-1}^1 \bar{B}^T \bar{E} \bar{B} |J| dr ds \quad (14)$$

which must be evaluated numerically.

Mass Matrix

The dynamics of elastic structures is based on Hamilton's variational principle with the kinetic energy of

$$\Pi_k = \frac{1}{2} \int_{\Omega} \dot{w}^T \mu \dot{w} d\Omega. \quad (15)$$

where w represents the vector of generalized displacement components relevant to inertial forces, the dot denotes the partial derivative with respect to time t , and μ is the mass density matrix of the form (Ayvaz et al., 1998)

$$\mu = \begin{bmatrix} m_1 & 0 & 0 \\ 0 & m_2 & 0 \\ 0 & 0 & m_3 \end{bmatrix}, \quad (16)$$

where $m_1 = \rho_p t$, $m_2 = m_3 = \frac{1}{12}(\rho_p t^3)$, and ρ_p is the mass density of the plate. Then the formula for the consistent mass matrix of the plate may be written as

$$M = \int_{\Omega} h_i^T \mu h_i d\Omega. \quad (17)$$

It should be noted that, in this study, the Newmark- β method is used for the time integration of Equation (1) by using the average acceleration method.

Numerical Examples

Data for numerical examples

In the light of the results given in reference (Özdemir et al., 2007), the aspect ratios, b/a , of the plate are taken to be 1, 1.5, and 2.0. The thickness/span ratios, t/a , are taken as 0.05, 0.1, and 0.2 for each aspect ratio. The shorter span length of the plate is kept constant to be 3 m. The mass density, Poisson's ratio, and the modulus of elasticity of the plate are taken to be $2.5 \text{ kN s}^2/\text{m}^2$, 0.2, $2.8 \times 10^7 \text{ kN/m}^2$, respectively. In order to obtain the response of each plate, the first 20 sn of YPT330 component the August 17, 1999 Kocaeli earthquake in Turkey is used since the peak value of the record occurred in this range (Figure 3).

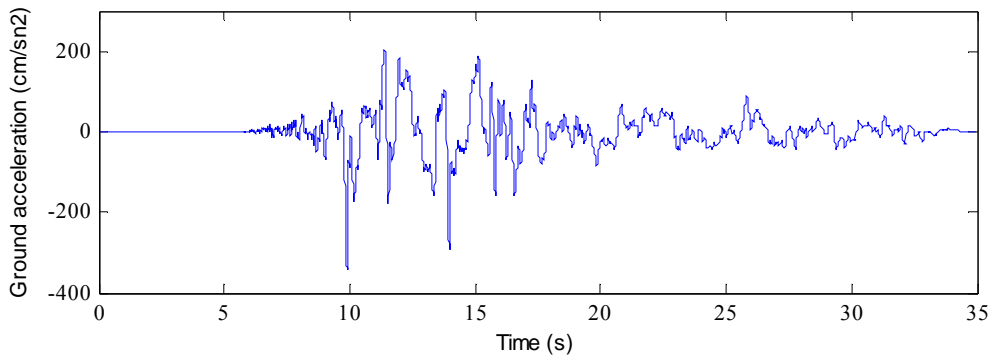


Figure 3. YPT330 component of the August 17, 1999 Kocaeli earthquake in Turkey

For the sake of accuracy in the results, rather than starting with a set of a finite element mesh size and time increment, the mesh size and time increment required to obtain the desired accuracy were determined before presenting any results. This analysis was performed separately for the mesh size and time increment. It was concluded that the results have acceptable error when equally spaced 16×16 mesh sizes are used for a 3 m x 3 m plate, if the 0.005 s time increment is used. Lengths of the elements in the y direction are kept constant for different aspect ratios.

Results

The purpose of this paper is to study shear locking-free analysis of thick plates subjected to earthquake excitations, to determine the effects of the thickness/span ratio, the aspect ratio and the boundary conditions on the linear responses of thick plates using Mindlin's theory, and to calculate the time histories of the displacements and bending moments at different points, but presentation of all of the time histories would take up excessive space. Hence, only the maximum displacements for different thickness/span ratios and the aspect ratios are presented after two time histories are given. This simplification of presenting only the maximum responses is supported by the fact that the maximum values of these quantities are the most important ones for design. These results are presented in graphical rather than in tabular form.

The time histories of the center displacements of the clamped plates are given in Figure 4 for $b/a=1.0$ and $t/a=0.05$, in Figure 5 for $b/a=1.0$ and $t/a=0.2$, and in Figure 6 for $b/a=2.0$ and $t/a=0.2$. As seen from these three figures, the center displacements of the clamped plates for $b/a = 1$, and $t/a = 0.05$, for $b/a = 1$, and $t/a = 0.2$, and for $b/a = 2$, and $t/a = 0.2$, reached their maximum values of 0.017 mm at 9.895 s, of 0.00164 mm at 9.895 s, and of 0.00298 mm at 9.895 s.

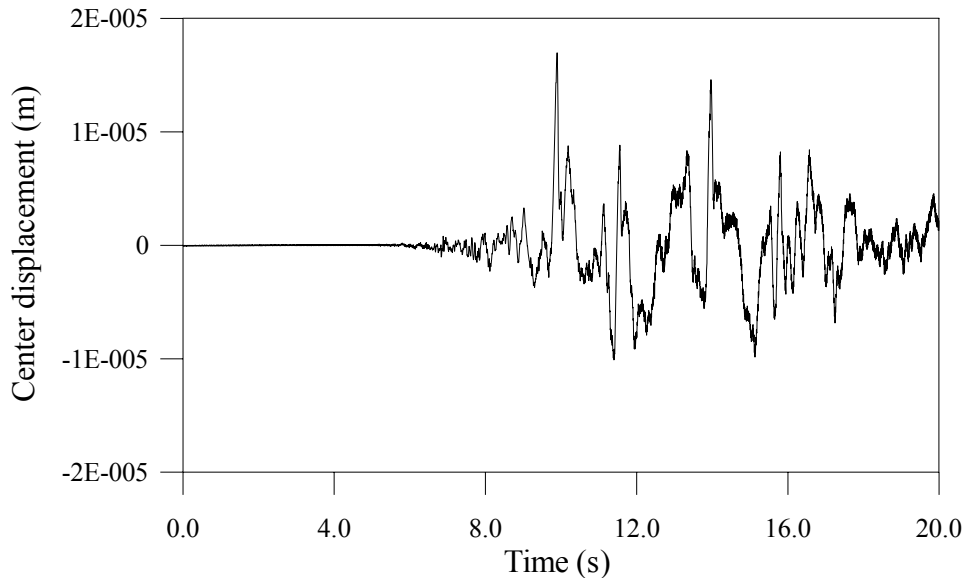


Figure 4. The time history of the center displacement of the clamped plate for $b/a=1.0$ and $t/a=0.05$.

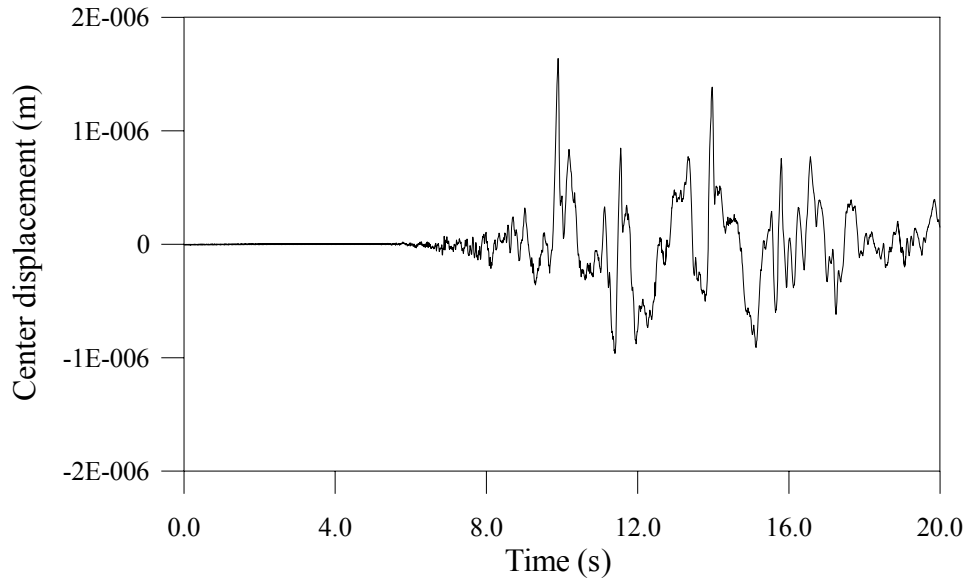


Figure 5. The time history of the center displacement of the clamped plate for $b/a=1.0$ and $t/a=0.2$.

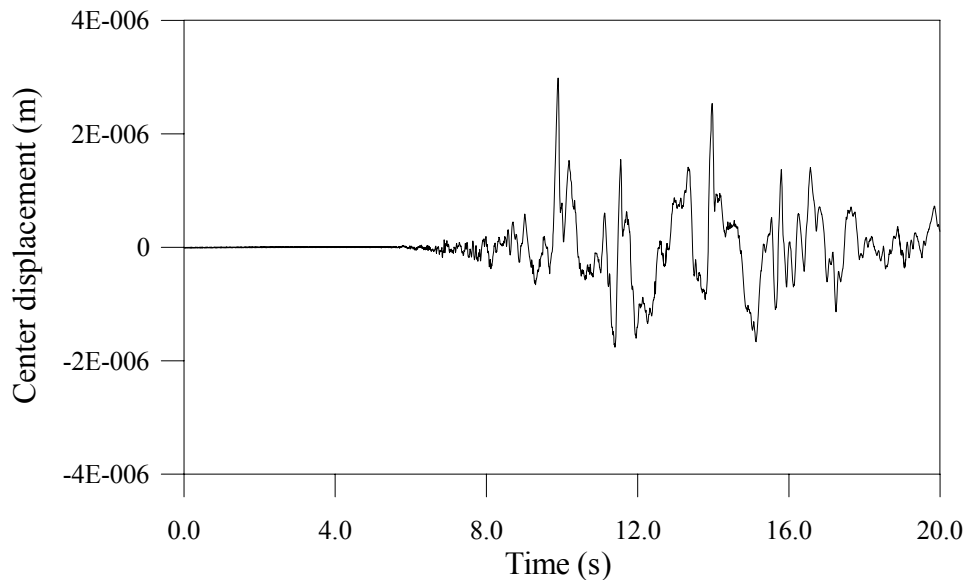


Figure 6. The time history of the center displacement of the clamped plate for $b/a=2.0$ and $t/a=0.2$.

The absolute maximum displacements of the plates for different aspect ratios, and thickness/span ratios are given in Figures 7, and 8 for the plates simply supported along all four edges, and for the plates clamped along all four edges, respectively.

As seen from Figures 7, and 8, the absolute maximum displacements of simply supported and clamped plates increase with increasing aspect ratio and decrease with increasing thickness/span ratio. The increase in the maximum displacement decreases with increasing aspect ratio. When the thickness/span ratio increases, the maximum displacements tend to level off. This means that the maximum displacement does not vary that much for the thicker plates as the aspect ratio increases. As also seen from these two figures, the maximum displacements of the simply supported plates are larger than those of the clamped plates for the same aspect and thickness/span ratios.

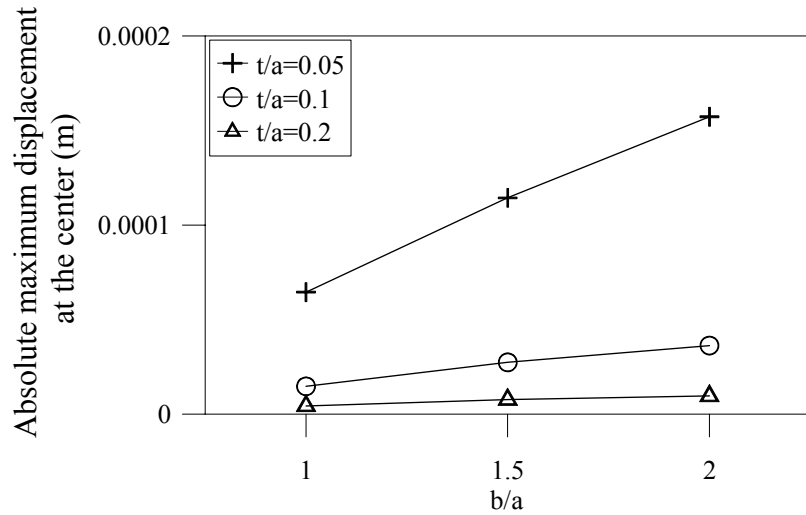


Figure 7. Absolute maximum displacement of the simply supported plates for different aspect ratios and thickness/span ratios.

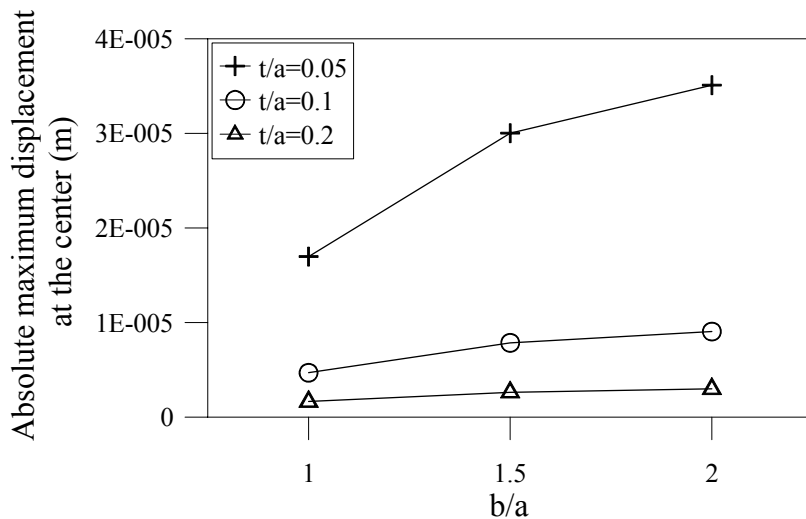


Figure 8. Absolute maximum displacement of the clamped plates for different aspect ratios and thickness/span ratios.

The absolute maximum bending moments M_x , and M_y at the center of the plates simply supported along all four edges for different aspect ratios, and thickness/span ratios are given in Figures 9, and 10, respectively.

As seen from Figure 9, the absolute maximum bending moments M_x at the center of simply supported plates increase with increasing aspect ratio and thickness/span ratio. The increase in the maximum bending moment M_x decreases with increasing aspect ratio, and increases with increasing thickness/span ratio.

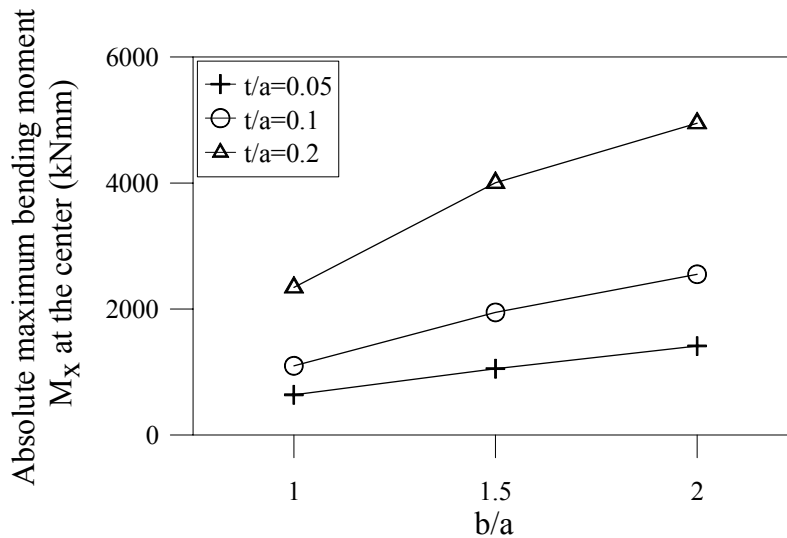


Figure 9. Absolute maximum bending moment M_x at the center of the simply supported plates for different aspect ratios and thickness/span ratios.

As seen from Figure 10, the absolute maximum bending moments M_y at the center of simply supported plates decrease with increasing aspect ratio and thickness/span ratio. The decrease in the maximum bending moment M_y increases with increasing aspect ratio, and decreases with decreasing thickness/span ratio.

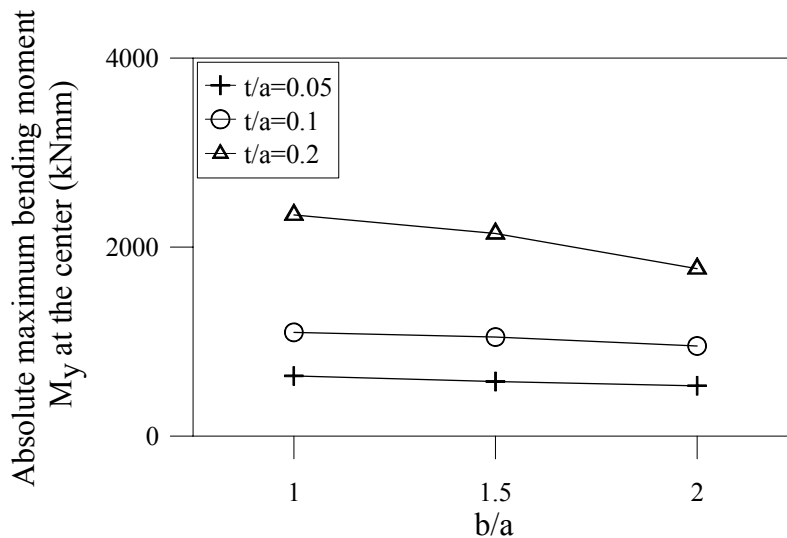


Figure 10. Absolute maximum bending moment M_y at the center of the simply supported plates for different aspect ratios and thickness/span ratios.

The absolute maximum bending moments M_x , and M_y at the center and at the center of the edges in the y and x directions for the plates clamped along all four edges are given in Figures 11, 12, 13, and 14, respectively, for different aspect ratios and thickness/span ratios.

As seen from Figure 11, as in the case of the absolute maximum bending moment M_x at the center of the simply supported plates, the absolute maximum bending moments M_x at the center of the clamped plates increase with increasing aspect ratio and thickness/span ratio. The increase in this maximum bending moment M_x decreases with increasing aspect ratio, and increases with increasing thickness/span ratio.

As seen from Figure 12, as in the case of the absolute maximum bending moment M_y at the center of the simply supported plates, the absolute maximum bending moments M_y at the center of clamped plates decrease with increasing aspect ratio and increase with increasing thickness/span ratio. The decrease in this maximum bending moment M_y increases with increasing aspect ratio and decreasing thickness/span ratio.

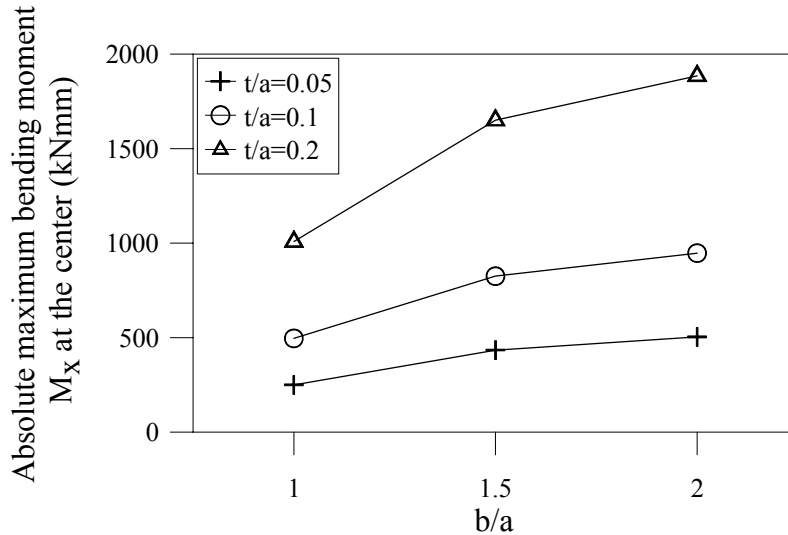


Figure 11. Absolute maximum bending moment M_x at the center of the clamped plates for different aspect ratios and thickness/span ratios.

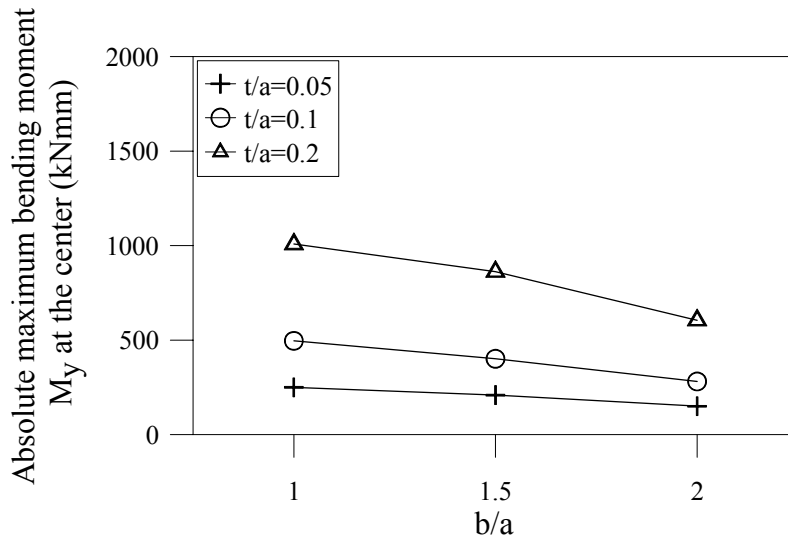


Figure 12. Absolute maximum bending moment M_y at the center of the clamped plates for different aspect ratios and thickness/span ratios.

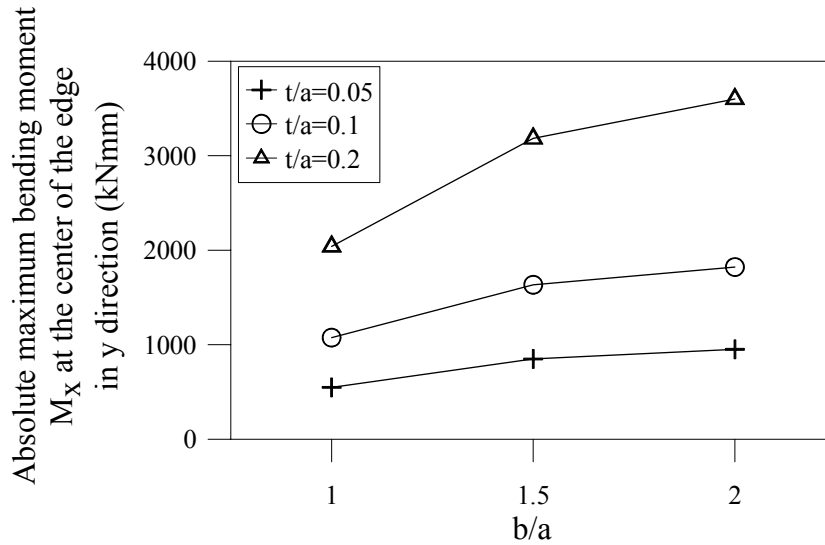


Figure 13. Absolute maximum bending moment M_x at the center of the edge in the y direction of the clamped plates for different aspect ratios and thickness/span ratios.

As seen from Figure 13, as in the case of the absolute maximum bending moment M_x at the center, the absolute maximum bending moments M_x at the center of the edge in the y direction of the clamped plates increase with increasing aspect ratio and thickness/span ratio. The degree of increases in this maximum bending moment M_x decreases with increasing aspect ratio, and increases with increasing thickness/span ratio.

As seen from Figure 14, the absolute maximum bending moments M_y at the center of the edge in the x direction of the clamped plates increase with increasing aspect ratio and thickness/span ratio. The increase in this maximum bending moment M_x is negligible for the large values of the aspect ratio for any values of the thickness/span ratios.

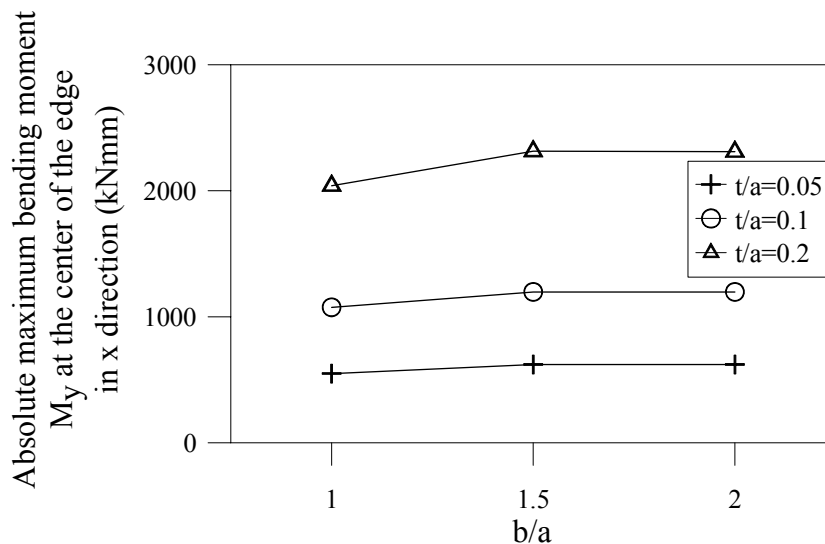


Figure 14. Absolute maximum bending moment M_y at the center of the edge in the x direction of the clamped plates for different aspect ratios and thickness/span ratios.

As also seen from these Figures the effects of the aspect ratios on the absolute maximum displacements and bending moments are larger for larger values of the thickness/span ratios than for smaller values of the thickness/span ratios. The effects of the thickness/span ratios on the absolute maximum displacement and bending moments are also larger for larger values of the aspect ratios than for smaller values of the aspect ratios.

The effects of the aspect and thickness/span ratios on the maximum responses considered in this study depend on the values of them. In general, the thickness/span ratio is more effective on the maximum responses than the aspect ratio.

Conclusions

The purpose of this paper was to study shear locking-free analysis of thick plates using Mindlin's theory by using 8-noded finite element and to determine the effects of the thickness/span ratio, the aspect ratio and the boundary conditions on the maximum displacements and bending moments of thick plates subjected to earthquake excitations. It is concluded, after comparisons are made with the results given in the literature, that by using 8-noded finite element, the mesh size required to produce the desired accuracy can be approximately reduced to 1/2 of those of the 4-noded finite elements. In addition, the following conclusions can also be drawn from the results obtained in this study.

The maximum displacements of the thick plates increase as the aspect ratio increases.

The bending moments M_x at the center of the plates increase with increasing aspect ratios.

The bending moments M_y at the center of the plates decrease with increasing aspect ratios.

The bending moments M_x at the center of the edge in the y direction of the clamped plates increase as the aspect ratio increases.

The bending moments M_y at the center of the edge in the x direction of the clamped plates almost remain the same as the aspect ratio increases.

Degree of decreases or increases decreases with increasing aspect ratios.

The effects of the aspect ratios on the absolute maximum displacements and bending moments are larger for larger values of the thickness/span ratios than for smaller values of the thickness/span ratios.

The effects of the thickness/span ratios on the absolute maximum displacement and bending moments are also larger for larger values of the aspect ratios than for smaller values of the aspect ratios.

The effects of the aspect and thickness/span ratios on the maximum responses considered in this study depend on the values of them.

In general, the thickness/span ratio is more effective on the maximum responses than the aspect ratio.

Acknowledgements

This study is supported by the Research Fund of Karadeniz Technical University. Project number: 2002.112.1.5.

References

- Ayvaz, Y., 1992, Parametric Analysis of Reinforced Concrete Slabs Subjected to Earthquake Excitation, Ph. D. Thesis, Graduate School of Texas Tech University, Lubbock, Texas.
- Cook, R.D., and Malkus, D.S. and Michael, E.P., 1989, Concepts and Applications of Finite Element Analysis, John Wiley & Sons, Inc., Canada.
- Mindlin, R.D., 1951, Influence of rotatory inertia and shear on flexural motions of isotropic, elastic plates, **Journal of Applied Mechanics**, 18, 31-38.
- Özdemir, Y. I., and Ayvaz, Y., 2004, Analysis of clamped and simply supported thick plates using finite element method, Proc. of the 6th Int. Cong. on Advances in Civil Engineering, İstanbul, 1: 652-661.
- Özdemir, Y. I., Bekiroğlu S., and Ayvaz, Y., 2007, Shear Locking-Free Analysis of Thick Plates Using Mindlin's Theory, **Structural Engineering and Mechanics**, 27(3).
- Özdemir, Y. I., and Ayvaz, Y., 2007, Shear Locking-Free Analysis of Thick Plates Subjected To Earthquake Excitations, *International Conference on Civil, Structural and Environmental Engineering Computing*, St. Julians, Malta, September, 212-227.
- Reissner, E., 1947, On bending of elastic plates, **Quarterly of Applied Mathematics**., 5, 55-68.
- Weaver, W., and Johnston, P.R. 1984, Finite Elements for Structural Analysis, Prentice Hall, Inc., Englewood Cliffs, New Jersey, 200-212.
- Y. Ayvaz, A. Daloğlu, A. Doğangün, 1998, Application of a Modified Vlasov Model to Earthquake Analysis of the Plates Resting on Elastic Foundations, **Journal of Sound and Vibration**, 499-509.